

MOLLIBRA: Genetic Molecular Optimization with Multi-Fingerprint Surrogates and Text-Molecule Aligned Critic

Masashi Okada¹ Kazuki Sakai¹ Hiroaki Yoshida¹ Masaki Okoshi¹ Tadahiro Taniguchi²

Abstract

We study sample-efficient molecular optimization under a limited budget of oracle evaluations. We propose MOLLIBRA (**M**ultim**O**da**L**ity and **L**anguage **I**ntegrated **B**ayesian and **e**volutiona**R**y optimiz**A**tion), a genetic algorithm based framework that pre-ranks candidate molecules using multiple critics before oracle calls: (i) an ensemble of Gaussian process (GP) surrogates defined over multiple molecular fingerprints and (ii) a pre-trained text-molecule aligned encoder CLAMP. The GP ensemble enables adaptive selection of task-appropriate fingerprints, while CLAMP provides a zero-shot scoring signal from task descriptions by measuring the similarity between molecular and text embeddings. On the Practical Molecular Optimization (PMO) benchmark with a budget of 1,000 evaluations (PMO-1K), MOLLIBRA- \mathcal{L} , our variant with a language-model-based candidate generator, attains the best Top-10 AUC on 14/22 tasks and the highest overall sum of Top-10 AUC across tasks among prior methods.

1. Introduction

Black-box optimization plays an essential role in molecular optimization applications such as drug design, and genetic algorithms (GAs) are a representative approach (Jensen, 2019; Moss et al., 2020; Tripp et al., 2021; Tripp & Hernández-Lobato, 2023; Kim et al., 2024; Wang et al., 2025a; Tripp & Hernández-Lobato, 2024; Yong et al., 2025; Lo et al., 2025). Compared to latent-space optimization methods (González-Duque et al., 2024; Moss et al., 2025; Boyar et al., 2025) that embed molecules into learned latent spaces using variational autoencoders (VAEs) (Kingma & Welling, 2013), GAs can directly search the space of molecular graphs or strings (e.g., SMILES (Weininger, 1988)). In addition, GA operations such as *crossover* and *mutation*

¹Panasonic Holdings Corp., Japan ²Kyoto University, Japan. Correspondence to: Masashi Okada <masashi.okada001@jp.panasonic.com>.

can incorporate chemical knowledge through graph-edit rule definitions (Jensen, 2019) or SMILES editing guided by large language models (LLMs) (Wang et al., 2025a). In practice, molecular optimization often operates under a limited number of oracle calls, typically on the order of hundreds (González-Duque et al., 2024; Moss et al., 2025; Boyar et al., 2025). This is because evaluating desired properties often requires complex simulations and/or wet-lab experiments, which can be time-consuming and costly (García-Ortegón et al., 2022; Stokes et al., 2020). However, many molecular optimization methods, including GA-based approaches, assume a large number of oracle calls (e.g., 10,000 calls) (Jensen, 2019; Tripp & Hernández-Lobato, 2023; 2024; Xu et al., 2024; Wang et al., 2025a; Lee et al., 2025), which is impractical in low-budget regimes.

We argue that GA performance in low-budget regimes is limited by the difficulty of constructing reliable surrogate models, due to (i) *fingerprint selection* and (ii) the *cold-start problem*. In the absence of surrogates to filter candidates (Jensen, 2019; Tripp & Hernández-Lobato, 2023; Wang et al., 2025a), GAs may conduct many wasteful evaluations. In contrast, some GA methods employ Gaussian process (GP) surrogates (Moss et al., 2020; Tripp & Hernández-Lobato, 2023; 2024; Yong et al., 2025). To define the GP models, these methods encode molecular structures into vector representations, namely *fingerprints* (Landrum, 2012; Adamczyk & Ludynia, 2024), to compute similarities between molecules via kernel functions. Although the optimal fingerprint for accurate prediction depends on the prediction target (Griffiths et al., 2023), prior GA work typically uses a single fixed fingerprint, which can degrade optimization performance. Furthermore, GP surrogates require a certain amount of scored data to become reliable, leading to the cold-start problem that wastes precious oracle calls.

To address these challenges, we introduce MOLLIBRA (**M**ultim**O**da**L**ity and **L**anguage **I**ntegrated **B**ayesian and **e**volutiona**R**y optimiz**A**tion), which augments GA search with (i) *multi-fingerprint* GP surrogates and (ii) a *text-molecule aligned critic* based on Contrastive Language-Assay-Molecule Pre-training (CLAMP) (Seidl et al., 2023) for zero-shot warm-starting (Fig. 1). Our main contributions are summarized as follows.

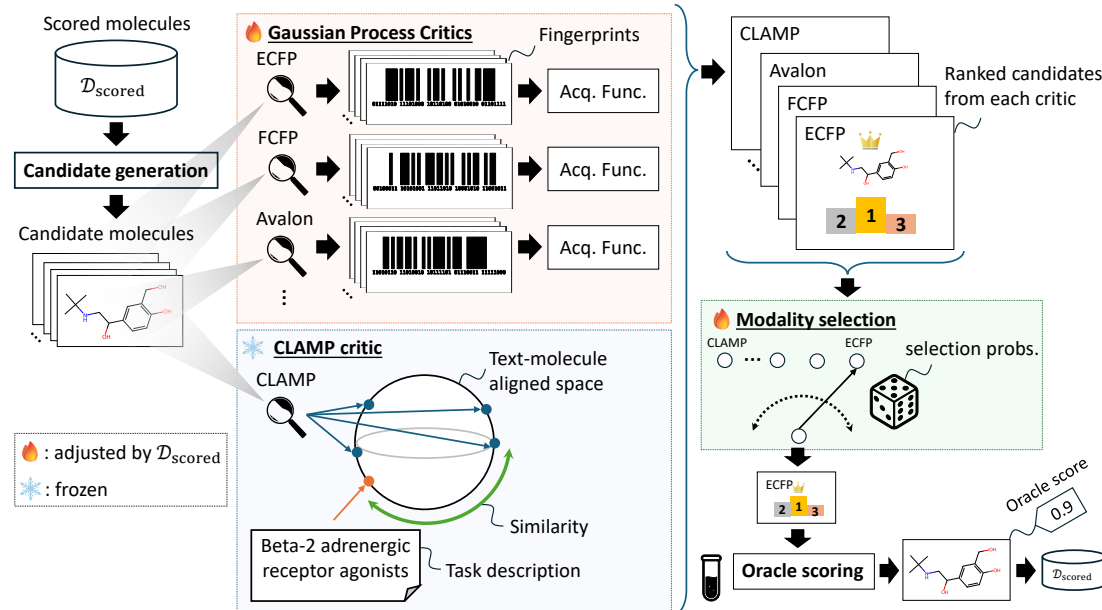


Figure 1. A conceptual illustration of MOLLIBRA, a GA-based molecular optimization framework with multi-fingerprint surrogates and a text-molecule-aligned critic. MOLLIBRA integrates two modalities for pre-evaluation: molecular fingerprints and natural-language task descriptions. The critics consist of learnable Gaussian process (GP) models defined over multiple fingerprints and a zero-shot critic based on a pretrained and frozen CLAMP model (Seidl et al., 2023). A critic is probabilistically selected for candidate ranking, and the selection probabilities are updated using the newly observed oracle scores.

- We introduce a *multi-fingerprint* surrogate ensemble: multiple structured-space GP models defined over different fingerprints to reduce sensitivity to fingerprint choice in low budgets.
- We integrate a *text-molecule aligned* critic from CLAMP (Seidl et al., 2023) to provide an early (zero-shot) ranking signal from task descriptions before sufficient scored data are available.
- On the Practical Molecular Optimization (PMO) benchmark (Gao et al., 2022) under the $N = 1,000$ budget setting, MOLLIBRA- \mathcal{L} , our variant with a language-model-based GA operator, achieves the best Top-10 AUC on 14/22 tasks, and attains the best overall sum of Top-10 AUC across tasks among the compared methods (Table 1).

The remainder of this paper is organized as follows. In Sec. 2, we provide preliminaries on molecular optimization and the building blocks of MOLLIBRA. In Sec. 3, we discuss key differences from related work. In Sec. 4, we present the details of MOLLIBRA. In Sec. 5, we empirically evaluate the performance of MOLLIBRA on the PMO benchmark. Finally, Sec. 6 concludes this paper.

2. Preliminaries

This section introduces the problem setup and the principal components of MOLLIBRA. We first formalize black-box molecular optimization, then review GA-based optimization. We also summarize GP surrogates, fingerprints, GP ensembles (Lu et al., 2023), and CLAMP (Seidl et al., 2023).

2.1. Black-box Optimization of Molecular Structures

The molecular structure optimization problem can be formulated as follows:

$$x^* = \arg \max_{x \in \mathcal{X}} F(x), \quad (1)$$

where $F : \mathcal{X} \rightarrow \mathbb{R}$ is an oracle function that evaluates specific properties of molecules (e.g., bioactivity, docking score), x represents a molecular structure (e.g., SMILES, graph), and \mathcal{X} is the set of structures. The goal is to find an optimal molecule $x^* \in \mathcal{X}$ within a limited oracle call budget N .

2.2. Molecular Optimization via Genetic Algorithm

The top-level pseudocode of a genetic algorithm (GA) for molecular optimization is presented in Alg. 1. This code generalizes existing and proposed GA-based molecular optimization methods by allowing various techniques to be represented through parameter settings and subroutine implementations.

Algorithm 1 GA-based molecular optimization.

Given: Budget N , Initial samples N_{init} , Batch size N_{batch} , Oracle function F ; Candidate pool size N_{cand}

- 1: **for** $n \in \{1, \dots, N_{\text{init}}\}$ **do** ▷ Initial sampling loop
- 2: $x_* \sim p_{\text{init}}(x)$ ▷ Sample from given molecular dataset
- 3: $\mathcal{D}_{\text{scored}} \leftarrow \mathcal{D}_{\text{scored}} \cup (x_*, y_* = F(x_*))$
- 4: **end for**
- 5: $n \leftarrow N_{\text{init}}$
- 6: $\mathcal{D}_{\text{cand}} \leftarrow \emptyset$ ▷ Initialize candidate pool
- 7: **while** True **do** ▷ Main loop
- 8: $\mathcal{D}_{\text{cand}} \leftarrow \mathcal{D}_{\text{cand}} \cup \text{GENOFFSPRING}(\mathcal{D}_{\text{scored}})$
- 9: $f \leftarrow \text{FITSURROGATE}(\mathcal{D}_{\text{scored}})$
- 10: $\mathcal{D}_{\text{sorted}} \leftarrow \text{PREEVALUATE}(\mathcal{D}_{\text{cand}}, f)$ ▷ Sort by pre-evaluated ranking using f
- 11: $\mathcal{D}_{\text{top}} \leftarrow \mathcal{D}_{\text{sorted}}[1:N_{\text{batch}}]$ ▷ Select top- N_{batch} samples
- 12: **for** $x_* \in \mathcal{D}_{\text{top}}$ **do** ▷ Oracle call loop
- 13: $\mathcal{D}_{\text{scored}} \leftarrow \mathcal{D}_{\text{scored}} \cup (x_*, y_* = F(x_*))$
- 14: $n \leftarrow n + 1$
- 15: **if** $n > N$ **then return** $\mathcal{D}_{\text{scored}}$
- 16: **end for**
- 17: $\mathcal{D}_{\text{sorted}} \leftarrow \mathcal{D}_{\text{sorted}} \setminus \mathcal{D}_{\text{top}}$ ▷ Remove scored samples
- 18: $\mathcal{D}_{\text{cand}} \leftarrow \mathcal{D}_{\text{sorted}}[1:N_{\text{cand}}]$ ▷ Keep candidate pool size
- 19: **end while**

In the main loop of Alg. 1, the GENOFFSPRING subroutine defined in Alg. 2 is called to generate new candidate molecules and add them to the candidate pool $\mathcal{D}_{\text{cand}}$. Within the GENOFFSPRING subroutine, the EDITMOL subroutine edits molecular structures in graph or string representations to perform crossover and mutation operations. GraphGA (Jensen, 2019) implements these editing operations using rule-based methods, whereas MOLLEO (Wang et al., 2025a) requests edits from an LLM. The pre-evaluation step in Alg. 1 ℓ9–11 prescreens candidates in $\mathcal{D}_{\text{cand}}$ using a surrogate model $f(x)$ fitted on the scored set $\mathcal{D}_{\text{scored}}$. Gaussian process regression, described in the next subsection, is widely used for constructing surrogate models $f(x)$. In Alg. 1 ℓ12–16, candidates in \mathcal{D}_{top} are evaluated using the oracle F , and the results are added to the observed data $\mathcal{D}_{\text{scored}}$. Some of the unevaluated candidates remain in $\mathcal{D}_{\text{cand}}$ and are subject to pre-evaluation again in the next generation (ℓ17–18).

2.3. Gaussian Process Models

A Gaussian process (GP) models the posterior distribution of a function $f(x)$ (a surrogate for the oracle F) conditioned on observed data $\mathcal{D} = \{(x, y = F(x))\}$;

$$p(f(x)|\mathcal{D}) = \mathcal{N}(f(x); \mu(x|\mathcal{D}), \sigma^2(x|\mathcal{D})), \quad (2)$$

where $\mu(\cdot)$ and $\sigma^2(\cdot)$ are the posterior mean and variance defined with a kernel function $k(x, x')$ that measures similarity between x and x' . Commonly used kernels include the Radial Basis Function (RBF) kernel and Matérn kernel defined in continuous spaces; however, applying these kernel functions to molecular structures is infeasible. Therefore,

Algorithm 2 GENOFFSPRING subroutine.

Given: Population size N_{elite} , Number of pairs N_{pairs} , Number of children (siblings) per pair N_{siblings}

- 1: **function** GENOFFSPRING($\mathcal{D}_{\text{scored}}$)
- 2: $\mathcal{D}_{\text{offspring}} \leftarrow \emptyset$
- 3: $\mathcal{D}_{\text{scored}} \leftarrow \text{SORTBYSCORES}(\mathcal{D}_{\text{scored}})$ ▷ Sort molecules by their oracle scores in desc. order
- 4: $\mathcal{D}_{\text{elite}} \leftarrow \mathcal{D}_{\text{scored}}[1:N_{\text{elite}}]$ ▷ Select top- N_{elite} molecules
- 5: **for** $i \in \{1, \dots, N_{\text{pairs}}\}$ **do**
- 6: $(x, x') \sim \text{SAMPLEPARENTS}(\mathcal{D}_{\text{elite}})$
- 7: $\{x_{\text{child}}\} \leftarrow \text{EDITMOL}(x, x', N_{\text{siblings}})$ ▷ Crossover and mutation yielding N_{siblings} children
- 8: $\mathcal{D}_{\text{offspring}} \leftarrow \mathcal{D}_{\text{offspring}} \cup \{x_{\text{child}}\}$
- 9: **end for**
- 10: **return** $\mathcal{D}_{\text{offspring}}$ ▷ Return $N_{\text{pairs}} \cdot N_{\text{siblings}}$ molecules
- 11: **end function**

vector representations of molecules, such as fingerprints, described in the next subsection, are employed. Hereafter, we refer to GPs based on fingerprints as *structured-space GPs*, following (Moss et al., 2025). In prior molecular optimization methods, acquisition functions such as Expected Improvement (EI) and Upper Confidence Bound (UCB) are computed for each candidate molecule using surrogate models to select candidates. In this study, we employ EI, defined as follows:

$$\alpha_{\text{EI}}(x|\mu, \sigma^2) \triangleq \mathbb{E}_{y \sim \mathcal{N}(y|\mu(x|\cdot), \sigma^2(x|\cdot))} [\max(0, y - y^*)], \quad (3)$$

where $y^* = \max_{y \in \mathcal{D}} y$.

2.4. Fingerprints and Their Similarity Measure

Molecular fingerprints are fixed-length vectors $x_f \in \mathbb{Z}^d$ derived from molecular structures that are directly input to machine learning models, including GPs. Each dimension of x_f represents the presence of specific substructures or chemical groups in the structure x as binary or count values. Different types of fingerprints can be obtained for the same molecular structure x depending on how substructures are defined (Landrum, 2012; Adamczyk & Ludynia, 2024), which represent the same molecule through different *lenses*. Prior molecular optimization studies (Tripp & Hernández-Lobato, 2023; 2024; Moss et al., 2025; Yong et al., 2025) conventionally use Extended-Connectivity Fingerprints (ECFP) (Rogers & Hahn, 2010), while evaluations with other fingerprints or combinations of multiple fingerprints remain underexplored in the molecular optimization literature.

As a kernel function measuring similarity between molecular fingerprints, Tanimoto similarity is widely used (Griffiths et al., 2023; Tripp & Hernández-Lobato, 2024; Moss et al.,

2025; Yong et al., 2025; Nguyen & Grover, 2025):

$$k(x_f, x'_f) = \frac{x_f \cdot x'_f}{\|x_f\|^2 + \|x'_f\|^2 - x_f \cdot x'_f}, \quad (4)$$

which is equivalent to the well-known Jaccard index, representing the ratio of the intersection to the union.

2.5. Ensemble of GP Models

(Lu et al., 2023) proposed an ensemble of GP models to improve robustness to kernel selection in Bayesian optimization. In this method, M models with different kernels $\{p(f_m | \cdot) = \mathcal{N}(f_m; \mu_m, \sigma_m^2)\}_{m=1}^M$ are constructed, each assigned a selection probability w_m . This selection probability is updated based on the likelihood of each model whenever a new observation $(x_*, y_*) \notin \mathcal{D}$ is obtained:

$$w_m \leftarrow w_m \cdot \mathcal{N}(y_*; \mu_m(x_* | \mathcal{D}), \sigma_m^2(x_* | \mathcal{D})) \cdot Z^{-1}, \quad (5)$$

where Z is a normalization constant ensuring $\sum w_m = 1$. During the computation of the acquisition function, a single model is selected based on these selection probabilities. This approach enables online selection of kernels suitable for a current task.

2.6. CLAMP

CLAMP (Contrastive Language-Assay-Molecule Pre-training) (Seidl et al., 2023) applies the concept of CLIP (Radford et al., 2021), a well-known image-text aligned embedding model, to cheminformatics through contrastive pre-training of molecule $x \in \mathcal{X}$ and assay text $a \in \mathcal{S}$ pairs, where \mathcal{S} is the set of natural language strings. CLAMP employs a molecule encoder $q_{\text{mol}}: \mathcal{X} \rightarrow \mathbb{R}^{768}$ and a text encoder $q_{\text{text}}: \mathcal{S} \rightarrow \mathbb{R}^{768}$, trained so that active molecule-text pairs yield high similarity scores $q_{\text{mol}}(x) \cdot q_{\text{text}}(a) \in \mathbb{R}$. Pretrained on massive molecular and bioassay text data from PubChem (Kim et al., 2023), CLAMP can score molecules for unseen assays described in natural language, enhancing zero-shot activity prediction performance.

3. Related Work

The most relevant works are Tripp’s GP Bayesian Optimization (BO) (Tripp et al., 2021) and its improved version (Tripp & Hernández-Lobato, 2024). (Tripp et al., 2021) has proposed a combination of GraphGA (Jensen, 2019) and a structured-space GP surrogate, and (Tripp & Hernández-Lobato, 2024) has reported performance improvements through the appropriate selection of fingerprints and scaling of kernel functions. MOLLIBRA builds on this line of work by using diverse fingerprints and incorporating a zero-shot text-molecule aligned critic.

COWBOYS (Moss et al., 2025) is a different type of molecular optimization method that uses structured-space GPs

as surrogates, while candidate generation is conducted in latent spaces obtained via VAEs (Kingma & Welling, 2013). BOSS (Moss et al., 2020) also combines GA and GP, but the GP is based on SMILES strings, and candidates are generated through string-level GA operations. GNN-SS and Gradient GA (Wang-Henderson et al., 2023; Mukherjee et al., 2025) construct surrogate models by using graph neural networks (GNNs). Latent-space Bayesian optimization methods (González-Duque et al., 2024; Moss et al., 2025; Boyar et al., 2025), which construct GPs and generate candidates in latent spaces, have been widely studied for molecular optimization.

Recently, methods that use *generative models*, in particular large language models (LLMs), for molecular optimization have gained attention. MOLLEO (Wang et al., 2025a), f-RAG (Lee et al., 2024), and GP-MolFormer-SIM (Navratil et al., 2026) use LLMs to generate molecular candidates. MOLLEO (Wang et al., 2025a) delegates GA’s crossover and mutation operations to LLMs. f-RAG uses retrieval-augmented generation (Lewis et al., 2020), and GP-MolFormer-SIM (Navratil et al., 2026) generates molecules through test-time guidance. Molecular graph generation methods based on diffusion models have also been recently proposed (Liu et al., 2025; Kaech et al., 2025; Lee et al., 2025). In principle, these generation methods can be combined with the proposed pre-evaluation mechanism; in our experiments, we adopt MOLLEO as a candidate generation engine. On the other hand, LICO (Nguyen & Grover, 2025) uses LLMs as critics, predicting oracle scores through in-context learning (Dong et al., 2024). MT-MOL (Kim et al., 2025) employs LLMs for both generation and pre-evaluation.

Reinforcement learning-based molecular optimization methods (Olivecrona et al., 2017; Ghugare et al., 2024; Xu et al., 2024; Hou, 2025; Wang et al., 2025b), represented by REINVENT (Olivecrona et al., 2017), treat molecular generative models as policies and optimize them using oracle scores as rewards. GFlowNets (Bengio et al., 2023) are methods for sampling molecules from an unnormalized reward-based probability distribution $\propto e^{F(x)}$, and Genetic GFN (Kim et al., 2024) is their application to molecular optimization. MARS (Xie et al., 2021) is another method for sampling molecules from unnormalized reward-based distributions, employing GNNs and Markov chain Monte Carlo sampling.

4. Method

This section describes the proposed method, MOLLIBRA, whose algorithm is presented in Algs. 3, 4, and 5. The top-level description shown in Alg. 3 is almost the same as Alg. 1, so we omit the initialization loop and highlight the different lines from Alg. 1. A distinctive feature of

Table 1. Top-10 AUC across methods on the PMO-1K benchmark (budget $N = 1,000$). We report mean \pm standard deviation over $n = 5$ seeds. For each task, the best and second-best scores are highlighted in **bold** and underline, respectively.

	Graph GA (Jensen, 2019)	REINVENT (Olivercrona et al., 2017)	LICO (Nguyen & Grover, 2025)	Genetic GFN (Kim et al., 2024)	MolLEO (Wang et al., 2025a)	Tripp's GP BO (Tripp & Hernández-Lobato, 2024)	MOLLIBRA- \mathcal{G} (ours)	MOLLIBRA- \mathcal{L} (ours)
albuterol_similarity	0.583 \pm 0.065	0.496 \pm 0.020	0.656 \pm 0.125	0.664 \pm 0.054	0.770 \pm 0.097	0.847 \pm 0.031	0.904 \pm 0.016	0.974 \pm 0.007
amlodipine_mpo	0.501 \pm 0.016	0.472 \pm 0.008	0.541 \pm 0.026	0.534 \pm 0.019	0.529 \pm 0.023	0.555 \pm 0.053	0.578 \pm 0.044	<u>0.619</u> \pm 0.058
celexcoxib_rediscovery	0.424 \pm 0.049	0.370 \pm 0.029	0.447 \pm 0.073	0.447 \pm 0.028	0.365 \pm 0.043	0.471 \pm 0.073	0.418 \pm 0.029	<u>0.709</u> \pm 0.068
deco_hop	0.581 \pm 0.006	0.572 \pm 0.006	0.596 \pm 0.010	0.604 \pm 0.017	0.603 \pm 0.013	0.605 \pm 0.003	0.635 \pm 0.009	<u>0.633</u> \pm 0.020
drd2_docking	0.833 \pm 0.065	0.775 \pm 0.086	0.859 \pm 0.066	0.809 \pm 0.045	0.951 \pm 0.010	0.551 \pm 0.477	0.867 \pm 0.167	<u>0.967</u> \pm 0.010
fenofenadine_mpo	0.666 \pm 0.009	0.650 \pm 0.007	0.700 \pm 0.023	0.682 \pm 0.021	0.714 \pm 0.009	0.755 \pm 0.026	<u>0.782</u> \pm 0.011	0.741 \pm 0.032
gsk3_beta	0.523 \pm 0.047	0.589 \pm 0.063	0.617 \pm 0.063	0.637 \pm 0.018	0.631 \pm 0.126	0.477 \pm 0.092	0.520 \pm 0.056	<u>0.723</u> \pm 0.067
isomer_c7h8n2o2	0.735 \pm 0.112	0.725 \pm 0.064	0.779 \pm 0.099	0.738 \pm 0.039	0.603 \pm 0.117	0.890 \pm 0.036	0.905 \pm 0.034	0.841 \pm 0.030
isomer_c9h10n2o2pf2cl	0.630 \pm 0.086	0.630 \pm 0.032	0.672 \pm 0.075	0.656 \pm 0.075	0.601 \pm 0.161	0.819 \pm 0.059	0.818 \pm 0.053	<u>0.828</u> \pm 0.034
jnk3	0.301 \pm 0.071	0.315 \pm 0.042	0.336 \pm 0.051	0.409 \pm 0.165	0.359 \pm 0.106	0.398 \pm 0.175	0.376 \pm 0.156	<u>0.495</u> \pm 0.065
median_1	0.208 \pm 0.015	0.205 \pm 0.012	0.217 \pm 0.019	0.219 \pm 0.008	0.157 \pm 0.015	0.331 \pm 0.009	<u>0.335</u> \pm 0.010	0.263 \pm 0.037
median_2	0.181 \pm 0.009	0.188 \pm 0.010	0.193 \pm 0.009	0.204 \pm 0.011	0.207 \pm 0.009	0.225 \pm 0.022	0.222 \pm 0.022	<u>0.282</u> \pm 0.015
mestranol_similarity	0.362 \pm 0.017	0.379 \pm 0.026	0.423 \pm 0.016	0.414 \pm 0.022	0.389 \pm 0.034	0.556 \pm 0.045	0.730 \pm 0.125	<u>0.630</u> \pm 0.150
osimetrinib_mpo	0.751 \pm 0.005	0.737 \pm 0.007	0.759 \pm 0.008	0.763 \pm 0.008	0.795 \pm 0.010	0.748 \pm 0.045	0.765 \pm 0.014	<u>0.828</u> \pm 0.021
perindopril_mpo	0.435 \pm 0.016	0.404 \pm 0.009	0.473 \pm 0.030	0.462 \pm 0.033	0.469 \pm 0.013	0.516 \pm 0.037	0.527 \pm 0.025	<u>0.526</u> \pm 0.019
rdkit_qed	0.914 \pm 0.007	0.921 \pm 0.002	0.925 \pm 0.005	0.928 \pm 0.002	0.926 \pm 0.009	0.929 \pm 0.006	0.928 \pm 0.007	<u>0.932</u> \pm 0.011
ranolazine_mpo	0.620 \pm 0.014	0.574 \pm 0.044	0.687 \pm 0.029	0.623 \pm 0.022	0.747 \pm 0.012	0.752 \pm 0.005	0.757 \pm 0.015	<u>0.777</u> \pm 0.021
scaffold_hop	0.461 \pm 0.008	0.447 \pm 0.010	0.480 \pm 0.008	0.485 \pm 0.015	0.491 \pm 0.055	0.495 \pm 0.015	0.555 \pm 0.014	<u>0.536</u> \pm 0.024
sitagliptin_mpo	0.229 \pm 0.053	0.261 \pm 0.026	0.315 \pm 0.097	0.227 \pm 0.041	0.258 \pm 0.087	0.353 \pm 0.125	0.424 \pm 0.110	<u>0.434</u> \pm 0.072
thiothixene_rediscovery	0.322 \pm 0.023	0.311 \pm 0.021	0.343 \pm 0.035	0.377 \pm 0.015	0.425 \pm 0.063	0.418 \pm 0.068	0.437 \pm 0.072	<u>0.615</u> \pm 0.017
troglitazone_rediscovery	0.267 \pm 0.015	0.246 \pm 0.009	0.292 \pm 0.028	0.277 \pm 0.015	0.271 \pm 0.010	0.459 \pm 0.048	0.451 \pm 0.061	0.412 \pm 0.084
zaleplon_mpo	0.374 \pm 0.024	0.406 \pm 0.017	0.404 \pm 0.022	0.400 \pm 0.014	0.405 \pm 0.018	0.419 \pm 0.024	0.443 \pm 0.031	<u>0.445</u> \pm 0.028
Sum	10.901	10.673	11.714	11.559	11.665	12.569	13.376	<u>14.208</u>

Algorithm 3 Main loop of MOLLIBRA.

Given: Budget N , Batch size N_{batch} , Candidate pool size N_{cand} , Oracle F , CLAMP encoders $q_{\text{mol}}, q_{\text{text}}$, Task description a

- $\{w_m\}_{m=1}^M \leftarrow 1/M$ \triangleright Initialize GP weights
- $\alpha_{\text{CLAMP}}(x) \triangleq q_{\text{mol}}(x) \cdot q_{\text{text}}(a)$ \triangleright Define zero-shot CLAMP critic
- while** True **do** \triangleright Main loop
- $\mathcal{D}_{\text{cand}} \leftarrow \mathcal{D}_{\text{cand}} \cup \text{GENOFFSPRING}(\mathcal{D}_{\text{scored}})$
- $\mathcal{F} \leftarrow \text{FITSURROGATE}(\mathcal{D}_{\text{scored}})$ $\triangleright \mathcal{F}$: a set of GPs over multiple fingerprints
- $\rho \leftarrow \text{CORR}(\{y\}_{y \in \mathcal{D}_{\text{scored}}}, \{\alpha_{\text{CLAMP}}(x)\}_{x \in \mathcal{D}_{\text{scored}}})$ \triangleright Calc. Spearman corr. b/w oracle and CLAMP scores
- $\mathcal{D}_{\text{sorted}} \leftarrow \text{PREEVALUATE}(\mathcal{D}_{\text{cand}}, \alpha_{\text{CLAMP}}, \rho, \mathcal{F}, \{w_m\})$
- $\mathcal{D}_{\text{top}} \leftarrow \mathcal{D}_{\text{sorted}}[1:N_{\text{batch}}]$
- for** $x_* \in \mathcal{D}_{\text{top}}$ **do** \triangleright Oracle call loop
- $\mathcal{D}_{\text{scored}} \leftarrow \mathcal{D}_{\text{scored}} \cup (x_*, y_* = F(x_*))$
- $n \leftarrow n + 1$
- if** $n > N$ **then return** $\mathcal{D}_{\text{scored}}$
- end for**
- $\{w_m\} \leftarrow \text{UPDATEGPWEIGHTS}(\mathcal{D}_{\text{scored}}, \mathcal{F})$ \triangleright Eq. (5)
- $\mathcal{D}_{\text{sorted}} \leftarrow \mathcal{D}_{\text{sorted}} \setminus \mathcal{D}_{\text{top}}$
- $\mathcal{D}_{\text{cand}} \leftarrow \mathcal{D}_{\text{sorted}}[1:N_{\text{cand}}]$
- end while**

MOLLIBRA is the use of multiple surrogates (or critics). By constructing and ensembling structured-space GPs over multiple fingerprint representations, we enhance robustness against uncertainty in molecular representations. We adopt an ensemble method from (Lu et al., 2023), which was originally developed for adaptive kernel selection. Additionally, by incorporating a zero-shot critic using CLAMP, we aim to improve optimization performance in low-budget regimes.

Algorithm 4 FITSURROGATE subroutine in MOLLIBRA.

Given: Fingerprint types $\{m\}_{m=1}^M$

- function** FITSURROGATE($\mathcal{D}_{\text{scored}}$)
- $\mathcal{F} \leftarrow \emptyset$
- for** Each fingerprint type $m = 1$ to M **do**
- $\mathcal{D}_{\text{scored}}^{(m)} \leftarrow \text{GETFINGERPRINT}(\mathcal{D}_{\text{scored}}, m)$
- $(\mu_m, \sigma_m^2) \leftarrow \text{FITGP}(\mathcal{D}_{\text{scored}}^{(m)})$
- $\mathcal{F} \leftarrow \mathcal{F} \cup \{(\mu_m, \sigma_m^2)\}$
- end for**
- return** \mathcal{F}
- end function**

4.1. Definition of Multiple Critics

The construction of multiple GP models is performed by the FITSURROGATE subroutine shown in Alg. 4, where molecules in $\mathcal{D}_{\text{scored}}$ are represented by M types of fingerprints, and one GP is constructed for each. The CLAMP critic is defined in Alg. 3 $\ell 2$, where a is a text that describes the desired molecule, such as $a = \text{"Inhibition of L-type calcium channel"}$. We use the official CLAMP model and weights¹.

4.2. Selection of Multiple Critics' Results

Multiple critics constructed in the previous section are selected based on probabilities denoted by $\{w_m\}_{m=1}^M$ and ρ . Here, $\{w_m\}_{m=1}^M$ are the weights for each GP model, which are initialized uniformly in Alg. 3 $\ell 1$ and then updated based on Eq. (5) ($\ell 14$) using newly acquired observations. The

¹<https://github.com/ml-jku/clamp/tree/main>.

Table 2. Ablation study of MOLLIBRA- \mathcal{G} and MOLLIBRA- \mathcal{L} under a budget of $N = 300$ evaluations on the PMO benchmark. We report Top-10 AUC in a similar format to Table 1.

	MOLLIBRA- \mathcal{G}				MOLLIBRA- \mathcal{L}			
Multi-fingerprint	✓	✓			✓	✓		
CLAMP critic	✓		✓		✓		✓	
albuterol_similarity	0.748 \pm 0.021	0.757 \pm 0.042	0.632 \pm 0.019	0.641 \pm 0.024	0.890 \pm 0.043	0.866 \pm 0.076	0.856 \pm 0.085	0.735 \pm 0.132
amlodipine_mpo	0.488 \pm 0.041	0.492 \pm 0.046	0.466 \pm 0.028	0.472 \pm 0.033	0.508 \pm 0.045	0.517 \pm 0.031	0.497 \pm 0.055	0.514 \pm 0.035
celecoxib_rediscovery	0.366 \pm 0.026	0.376 \pm 0.019	0.367 \pm 0.018	0.381 \pm 0.028	0.588 \pm 0.073	0.615 \pm 0.079	0.466 \pm 0.082	0.499 \pm 0.063
deco_hop	0.591 \pm 0.010	0.600 \pm 0.014	0.588 \pm 0.011	0.589 \pm 0.005	0.597 \pm 0.012	0.599 \pm 0.015	0.591 \pm 0.015	0.585 \pm 0.005
drd2_docking	0.669 \pm 0.29	0.485 \pm 0.338	0.648 \pm 0.298	0.421 \pm 0.367	0.912 \pm 0.029	0.862 \pm 0.033	0.914 \pm 0.012	0.724 \pm 0.108
fenofenadine_mpo	0.689 \pm 0.039	0.658 \pm 0.069	0.625 \pm 0.057	0.649 \pm 0.061	0.689 \pm 0.040	0.664 \pm 0.035	0.663 \pm 0.059	0.668 \pm 0.070
gsk3_beta	0.333 \pm 0.054	0.361 \pm 0.059	0.365 \pm 0.052	0.319 \pm 0.077	0.564 \pm 0.050	0.463 \pm 0.084	0.626 \pm 0.125	0.505 \pm 0.062
isomer_c7h8n2o2	0.751 \pm 0.015	0.745 \pm 0.063	0.691 \pm 0.042	0.764 \pm 0.022	0.713 \pm 0.069	0.632 \pm 0.099	0.488 \pm 0.359	0.534 \pm 0.274
isomer_c9h10n2o2pf2cl	0.653 \pm 0.108	0.696 \pm 0.041	0.625 \pm 0.029	0.693 \pm 0.079	0.564 \pm 0.270	0.657 \pm 0.106	0.598 \pm 0.178	0.646 \pm 0.132
jnk3	0.234 \pm 0.070	0.244 \pm 0.106	0.211 \pm 0.053	0.270 \pm 0.130	0.297 \pm 0.107	0.263 \pm 0.067	0.285 \pm 0.052	0.251 \pm 0.097
median_1	0.279 \pm 0.011	0.287 \pm 0.009	0.270 \pm 0.007	0.276 \pm 0.010	0.225 \pm 0.030	0.223 \pm 0.026	0.192 \pm 0.032	0.192 \pm 0.026
median_2	0.193 \pm 0.026	0.194 \pm 0.025	0.191 \pm 0.019	0.197 \pm 0.021	0.230 \pm 0.018	0.222 \pm 0.026	0.212 \pm 0.015	0.230 \pm 0.039
mestranol_similarity	0.477 \pm 0.084	0.463 \pm 0.045	0.435 \pm 0.041	0.432 \pm 0.026	0.470 \pm 0.020	0.456 \pm 0.053	0.430 \pm 0.054	0.421 \pm 0.083
osimetrinib_mpo	0.708 \pm 0.024	0.700 \pm 0.027	0.698 \pm 0.040	0.700 \pm 0.044	0.750 \pm 0.039	0.739 \pm 0.050	0.736 \pm 0.034	0.740 \pm 0.020
perindopril_mpo	0.455 \pm 0.026	0.450 \pm 0.026	0.425 \pm 0.006	0.432 \pm 0.029	0.483 \pm 0.024	0.481 \pm 0.020	0.450 \pm 0.045	0.455 \pm 0.034
ranolazine_mpo	0.653 \pm 0.012	0.640 \pm 0.014	0.669 \pm 0.027	0.651 \pm 0.011	0.689 \pm 0.029	0.709 \pm 0.025	0.695 \pm 0.030	0.697 \pm 0.029
rdkit_qed	0.903 \pm 0.014	0.906 \pm 0.013	0.901 \pm 0.009	0.903 \pm 0.014	0.923 \pm 0.006	0.915 \pm 0.012	0.917 \pm 0.011	0.921 \pm 0.005
scaffold_hop	0.483 \pm 0.002	0.504 \pm 0.020	0.471 \pm 0.011	0.473 \pm 0.014	0.484 \pm 0.013	0.482 \pm 0.008	0.458 \pm 0.013	0.458 \pm 0.014
sitagliptin_mpo	0.236 \pm 0.063	0.236 \pm 0.067	0.144 \pm 0.090	0.174 \pm 0.157	0.298 \pm 0.056	0.300 \pm 0.080	0.287 \pm 0.091	0.348 \pm 0.053
thiothixene_rediscovery	0.326 \pm 0.036	0.356 \pm 0.051	0.309 \pm 0.037	0.316 \pm 0.044	0.480 \pm 0.079	0.445 \pm 0.041	0.440 \pm 0.044	0.470 \pm 0.072
troglitazone_rediscovery	0.316 \pm 0.031	0.335 \pm 0.030	0.319 \pm 0.019	0.334 \pm 0.018	0.310 \pm 0.030	0.312 \pm 0.033	0.302 \pm 0.027	0.309 \pm 0.036
zaleplon_mpo	0.386 \pm 0.026	0.382 \pm 0.025	0.311 \pm 0.032	0.350 \pm 0.040	0.394 \pm 0.053	0.400 \pm 0.037	0.367 \pm 0.055	0.403 \pm 0.039
Sum	10.934	10.868	10.362	10.439	12.058	11.823	11.469	11.306

Algorithm 5 PREEVALUATE subroutine in MOLLIBRA.

```

1: function PREEVALUATE( $\mathcal{D}_{\text{cand}}$ ,  $\alpha_{\text{CLAMP}}$ ,  $\rho$ ,  $\mathcal{F}$ ,  $\{w_m\}$ )
2:    $\mathcal{D}_{\text{sorted}} \leftarrow \emptyset$ 
3:   while  $\mathcal{D}_{\text{cand}} \neq \emptyset$  do            $\triangleright$  While candidates remain
4:      $u \sim U(0, 1)$                        $\triangleright$  Uniform random number
5:     if  $u < \text{CLIP}(\rho, 0, 1)$  then
6:        $x_* \leftarrow \arg \max_{x \in \mathcal{D}_{\text{cand}}} \alpha_{\text{CLAMP}}(x)$ 
7:     else
8:        $m \sim \text{Cat}(\{w_m\})$             $\triangleright$  Select GP index
9:        $\mathcal{D}_{\text{cand}}^{(m)} \leftarrow \text{GETFINGERPRINT}(\mathcal{D}_{\text{cand}}, m)$ 
10:       $x_* \leftarrow \arg \max_{x_f^{(m)} \in \mathcal{D}_{\text{cand}}^{(m)}} \alpha_{\text{EI}}(x_f^{(m)} | \mathcal{F}[m])$ 
11:    end if
12:     $\mathcal{D}_{\text{cand}} \leftarrow \mathcal{D}_{\text{cand}} \setminus \{x_*\}$   $\triangleright$  Remove selected sample
13:     $\mathcal{D}_{\text{sorted}} \leftarrow \mathcal{D}_{\text{sorted}} \cup \{x_*\}$ 
14:   end while
15:   return  $\mathcal{D}_{\text{sorted}}$ 
16: end function

```

value ρ computed in Alg. 3 $\ell 6$ is the Spearman correlation coefficient $\rho \in [-1, 1]$ between the oracle scores and CLAMP critic values in the evaluated data $\mathcal{D}_{\text{scored}}$. ρ is used as a gating probability to select between CLAMP and the GP models. Unlike GPs, CLAMP cannot evaluate the likelihood of new data as in Eq. (5); therefore, we use the correlation coefficient instead.

Based on the aforementioned selection probabilities, candidates in $\mathcal{D}_{\text{cand}}$ are ranked and sorted by the PREEVALUATE subroutine shown in Alg. 5. Here, a critic is probabilistically selected for each rank, and the result of that critic is adopted. We expect that switching critics within the loop will help

ensure diversity in the candidate pool $\mathcal{D}_{\text{cand}}$. The CLAMP critic is selected based on ρ clipped to $[0, 1]$. If CLAMP is not selected, a GP model is selected based on the probability distribution $\{w_m\}_{m=1}^M$, and the candidate that maximizes the acquisition function $\alpha_{\text{EI}}(x | \mu_m, \sigma_m^2)$ based on that GP is selected.

4.3. Implementation Details

Fingerprints, kernels and GP models In this paper, we adopt $M = 6$ types of fingerprints: ECFP, FCFP (Functional Connectivity Fingerprint) (Rogers & Hahn, 2010), Avalon (Gedeck et al., 2006), Pharmacophore (McGregor & Muskal, 1999), MAP (MinHashed Atom Pair) (Orsi & Reymond, 2024), and BoC (Bag-of-Characters) (Griffiths et al., 2023). BoC is a vector representation that counts the frequency of occurrence of characters contained in the SMILES string of a molecule; although it is not strictly a fingerprint, we treat it as a type of fingerprint in this paper. For all these fingerprints, we adopt the Tanimoto kernel defined in Eq. (4). We perform training and inference of the GP models using BoTorch (Balandat et al., 2020).

Candidate generation In this paper, we integrate both GraphGA’s graph editing (Jensen, 2019) and MOLLEO’s LLM-based SMILES generation (Wang et al., 2025a) into MOLLIBRA to realize the EDITMOL subroutine; these implementations are denoted as MOLLIBRA- \mathcal{G} and MOLLIBRA- \mathcal{L} , respectively. The LLM we use is GPT-5-mini (OpenAI, 2025), and the prompt for molecular editing is shown in Appendix List 1. Sampling from $p_{\text{init}}(x)$ in the

Table 3. Task description examples provided to CLAMP. One example is given for each of the three task categories. The definition rules for task descriptions in this paper and full version of this table are provided in Appendix A.2 and Table 5.

Category	Example of Task description <i>a</i>
(i) Drug-Effect Opt.	“Beta-2 adrenergic receptor agonists” (from <code>albuterol_similarity</code>)
(ii) Property Opt.	“Quantitative Estimate of Drug-likeness” (from <code>rdkit_qed</code>)
(iii) Structure-Constrained Opt.	“” (empty string) (from <code>deco_hop</code>)

initialization loop is performed by random selection from the ZINC-250K dataset (Gómez-Bombarelli et al., 2018) as in MOLLEO. Hyperparameters related to candidate generation are detailed in Appendix Table 4.

5. Experiments

5.1. Settings

Molecular optimization tasks We evaluate on 22 selected optimization tasks from the PMO benchmark (Gao et al., 2022)², a standard benchmark suite for molecular optimization. To specifically evaluate performance under a low oracle budget, the oracle budget for each task is limited to $N = 1,000$ oracle calls; this setting is referred to as PMO-1K (Nguyen & Grover, 2025; Kim et al., 2025).

Task descriptions for LLM and CLAMP We classify the tasks into three categories and provide task descriptions to the LLM and CLAMP according to each category. The categories and examples of task descriptions are shown in Table 3.

Baselines We compare MOLLIBRA- $\{\mathcal{G}, \mathcal{L}\}$ against six representative methods in PMO, namely Tripp’s GP BO (Tripp & Hernández-Lobato, 2024), MOLLEO (Wang et al., 2025a), Genetic GFN (Kim et al., 2024), LICO (Nguyen & Grover, 2025), REINVENT (Olivecrona et al., 2017), and Graph GA (Jensen, 2019). We implement Tripp’s GP BO and MOLLEO as special cases of MOLLIBRA- $\{\mathcal{G}, \mathcal{L}\}$. Tripp’s GP BO uses a single fingerprint (ECFP) and disables CLAMP in MOLLIBRA- \mathcal{G} , which matches the improved version described in (Tripp & Hernández-Lobato, 2024). MOLLEO disables all critics in MOLLIBRA- \mathcal{L} , using the same prompt template as MOLLIBRA- \mathcal{L} . For the other baselines (i.e., Genetic GFN, LICO, REINVENT, and Graph GA), we cite results from a

²The PMO benchmark is commonly evaluated on 23 tasks; however, we exclude the `valsartan_smarts` task in our experiments. This task employs a sparse oracle that returns 0 unless a specific substructure CN(C=O)Cc1ccc(c2cccccc2)cc1 is present, and many methods have failed to optimize it. (Lo et al., 2025) points out that this task is ill-suited for benchmarking, and we follow their recommendation.

previous study (Nguyen & Grover, 2025).

Metrics We use the Top-10 AUC metric to evaluate optimization performance, which measures the area under the curve of the average of the top-10 highest oracle scores obtained up to each evaluation step. This metric reflects both the quality of the best-found molecules and the speed of optimization.

5.2. Results

Comparison with the baselines The purpose of this experiment is to compare our two variants, MOLLIBRA- \mathcal{G} and MOLLIBRA- \mathcal{L} , with leading baselines on PMO-1K. Table 1 presents the Top-10 AUC scores for each method across tasks. MOLLIBRA- \mathcal{G} and MOLLIBRA- \mathcal{L} achieve the best scores in 7 and 14 out of 22 tasks, respectively, showing consistent gains over all baselines. Tripp’s GP BO ranks third overall, outperforming LLM-based methods such as MOLLEO and LICO, which differs from the results reported in (Nguyen & Grover, 2025). This difference is likely due to (Nguyen & Grover, 2025) using an earlier GP BO implementation from (Tripp et al., 2021) instead of the improved version from (Tripp & Hernández-Lobato, 2024).

Ablation study The purpose of this ablation study is to evaluate the effectiveness and contributions of each component of MOLLIBRA. In this experiment, we evaluated three variants that remove either or both of the main components of the proposed method: multi-fingerprint and CLAMP critic. The variant without multi-fingerprint uses only a single fingerprint (ECFP). The variant that removes both from MOLLIBRA- \mathcal{G} corresponds to Tripp’s GP BO. The trial budget for this evaluation was set to $N = 300$ (PMO-300). Table 2 presents the results of the ablation study. Overall, removing either component can degrade performance on multiple tasks, indicating that both multi-fingerprint and CLAMP can be beneficial under low budgets.

Contribution analysis of critics The purpose of this analysis is to understand the behavior of each critic (structured-space GPs and the CLAMP critic) during optimization and to support the necessity of the proposed adaptive critic selection. The analysis here focuses on MOLLIBRA- \mathcal{L} . Figure 2 visualizes the *contributions* of each critic in the optimization process. Here, the contribution is measured as the accumulation of step-wise score improvement realized by each critic over the entire process and all seeds. This result indicates that the contributing fingerprints vary across tasks, and the CLAMP critic also contributes non-trivially in multiple tasks; e.g., `albuterol_similarity`, `drd2_docking` and `gsk3_beta`.

Figure 3 shows the temporal evolution of contributions in four representative tasks. In the upper row (`gsk3_beta`

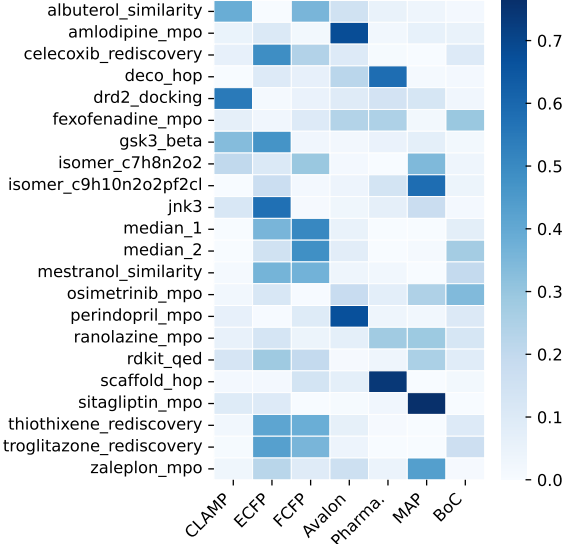


Figure 2. Heatmap visualizing the contribution of critics (structured-space GPs and the CLAMP critic) in MOLLIBRA- \mathcal{L} ’s optimization process. The color intensity indicates the accumulation of step-wise improvement in oracle scores realized by each critic. In the figure, the contributions are normalized so that the total contribution of all critics sums to 100%. Similar results for MOLLIBRA- \mathcal{G} are provided in Appendix Figure 4.

and jnk3), the CLAMP critic contributes most in the early steps. In contrast, there are tasks where CLAMP contributes negligibly in our runs (lower row: amlodipine_mpo and $\text{troglitazone_rediscovery}$), which we discuss in the next section. In $\text{troglitazone_rediscovery}$, FCFP takes over from ECFP as the main contributor around step 500, indicating that the contributions of fingerprints can change during the optimization process. Moreover, as shown in Appendix Figure 5, the contributions of critics can vary significantly across different seeds. This suggests that the effective fingerprints depend on the initial distribution of $\mathcal{D}_{\text{scored}}$. The above results indicate that it is challenging to select an effective single fingerprint in advance for specific tasks. We can therefore conclude that multi-fingerprint ensembling is essential.

Additional experiments Appendix B presents the results of various additional experiments, including extra contribution analyses and comparisons with latent-space optimization methods on PMO-300, which further support the effectiveness of MOLLIBRA. We also provide further ablation studies on MOLLIBRA’s components (i.e., GP ensemble and CLAMP gating method), where alternative components are evaluated to validate the design choices of the proposed method.

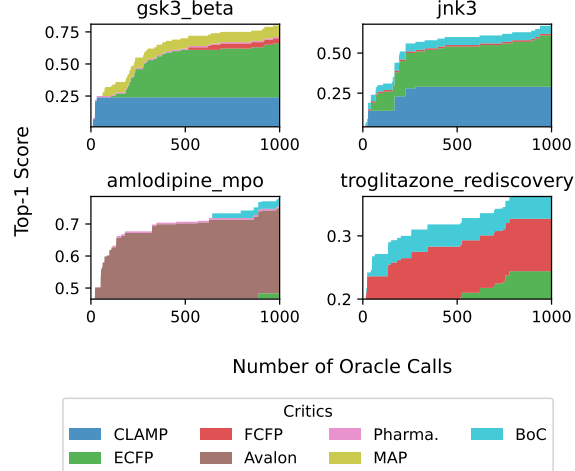


Figure 3. Temporal evolution of contributions in four tasks (results from a single seed run). The cumulative score improvement realized by each critic is shown as an area chart.

6. Discussion

We present MOLLIBRA, a GA-based molecular optimization method that combines an ensemble of structured-space GPs over multiple molecular fingerprints with a zero-shot CLAMP critic. Using multiple fingerprints improves robustness to representation choice, and incorporating CLAMP can strengthen performance in low-budget regimes. To our knowledge, this is the first work that incorporates both multi-fingerprint structured-space GPs and a CLAMP critic for molecular optimization, and it achieves the best overall Top-10 AUC among the compared methods on PMO-1K (Table 1).

A limitation of MOLLIBRA is that the CLAMP critic is not consistently helpful across tasks. One possible explanation is that CLAMP’s molecular encoder is based on ECFP-derived features (Seidl et al., 2023), which can overlap with information captured by ECFP-based GP critics. Since the most effective fingerprint differs across tasks, an ECFP-based CLAMP critic can be misaligned with the task-specific representation that best supports optimization.

Future work includes extending CLAMP to incorporate multiple fingerprint representations, which may improve its effectiveness as a zero-shot critic. Another direction is to expand the set of critics, for example by adding fingerprints not used in this study, using GP critics with the DICE kernel (Boyar et al., 2025) as an alternative to the Tanimoto kernel, or combining with LLM-based critics such as LICO (Nguyen & Grover, 2025).

References

Adamczyk, J. and Ludynia, P. Scikit-fingerprints: Easy and efficient computation of molecular fingerprints in python. *SoftwareX*, 28:101944, 2024.

Auer, P., Cesa-Bianchi, N., Freund, Y., and Schapire, R. E. The nonstochastic multiarmed bandit problem. *SIAM journal on computing*, 32(1):48–77, 2002.

Balandat, M., Karrer, B., Jiang, D., Daulton, S., Letham, B., Wilson, A. G., and Bakshy, E. Botorch: A framework for efficient monte-carlo bayesian optimization. *Advances in neural information processing systems*, 2020.

Bengio, Y., Lahlou, S., Deleu, T., Hu, E. J., Tiwari, M., and Bengio, E. GFlowNet foundations. *Journal of Machine Learning Research*, 24(210):1–55, 2023.

Berryman, J. and Ziegler, A. *Prompt Engineering for LLMs: The Art and Science of Building Large Language Model-Based Applications*. "O'Reilly Media, Inc.", 2024.

Boyar, O., Hanada, H., and Takeuchi, I. Conditional latent space molecular scaffold optimization for accelerated molecular design. *Transactions on Machine Learning Research*, 2025.

Cao, Y. and Fleet, D. J. Generalized product of experts for automatic and principled fusion of gaussian process predictions. In *Automating the Learning Pipeline workshop at NIPS 2014*, 2014.

Chang, C.-Y., Azvar, M., Okwudire, C., and Kontar, R. A. LLINBO: Trustworthy llm-in-the-loop bayesian optimization. *arXiv preprint arXiv:2505.14756*, 2025.

Dong, Q., Li, L., Dai, D., Zheng, C., Ma, J., Li, R., Xia, H., Xu, J., Wu, Z., Chang, B., et al. A survey on in-context learning. In *Proceedings of the 2024 conference on empirical methods in natural language processing*, pp. 1107–1128, 2024.

Gao, W., Fu, T., Sun, J., and Coley, C. W. Sample efficiency matters: A benchmark for practical molecular optimization. In *Advances in Neural Information Processing Systems*, volume 35, pp. 21342–21357. Curran Associates, Inc., 2022.

García-Ortegón, M., Simm, G. N. C., Tripp, A. J., Hernández-Lobato, J. M., Bender, A., and Bacallado, S. Dockstring: Easy molecular docking yields better benchmarks for ligand design. *Journal of Chemical Information and Modeling*, 62(15):3486–3502, 2022. doi: 10.1021/acs.jcim.1c01334.

Gedeck, P., Rohde, B., and Bartels, C. Qsar- how good is it in practice? comparison of descriptor sets on an unbiased cross section of corporate data sets. *Journal of chemical information and modeling*, 46(5):1924–1936, 2006.

Ghugare, R., Miret, S., Hugessen, A., Phiellip, M., and Berseth, G. Searching for high-value molecules using reinforcement learning and transformers. In *International Conference on Learning Representations*, 2024.

Gómez-Bombarelli, R., Wei, J. N., Duvenaud, D., Hernández-Lobato, J. M., Sánchez-Lengeling, B., Sheberla, D., Aguilera-Iparraguirre, J., Hirzel, T. D., Adams, R. P., and Aspuru-Guzik, A. Automatic chemical design using a data-driven continuous representation of molecules. *ACS central science*, 4(2):268–276, 2018.

González-Duque, M., Michael, R., Bartels, S., Zainchkovskyy, Y., Hauberg, S., and Boomsma, W. A survey and benchmark of high-dimensional bayesian optimization of discrete sequences. In *Advances in Neural Information Processing Systems*, 2024.

Griffiths, R.-R., Klarner, L., Moss, H. B., Ravuri, A., Truong, S., Stanton, S., Tom, G., Rankovic, B., Du, Y., Jamasb, A., Deshwal, A., Schwartz, J., Tripp, A., Kell, G., Frieder, S., Bourached, A., Chan, A., Moss, J., Guo, C., Durholt, J. P., Chaurasia, S., Strieth-Kalthoff, F., Lee, A. A., Cheng, B., Aspuru-Guzik, A., Schwaller, P., and Tang, J. Gauche: A library for gaussian processes in chemistry. In *Advances in Neural Information Processing Systems*, 2023.

Hou, J. De novo molecular design enabled by direct preference optimization and curriculum learning. In *Joint European Conference on Machine Learning and Knowledge Discovery in Databases*, pp. 95–111. Springer, 2025.

Jensen, J. H. A graph-based genetic algorithm and generative model/monte carlo tree search for the exploration of chemical space. *Chemical Science*, 2019.

Kaech, B., Wyss, L., Borgwardt, K., and Grasso, G. Refine drugs, don't complete them: Uniform-source discrete flows for fragment-based drug discovery. In *The NeurIPS 2025 Workshop on AI Virtual Cells and Instruments*, 2025.

Kim, H., Kim, M., Choi, S., and Park, J. Genetic-guided GFlowNets for sample efficient molecular optimization. *Advances in Neural Information Processing Systems*, 37: 42618–42648, 2024.

Kim, H., Jang, Y., and Ahn, S. MT-mol: Multi agent system with tool-based reasoning for molecular optimization. In *Empirical Methods in Natural Language Processing*, 2025.

Kim, S., Chen, J., Cheng, T., Gindulyte, A., He, J., He, S., Li, Q., Shoemaker, B. A., Thiessen, P. A., Yu, B., Zaslavsky, L., Zhang, J., and Bolton, E. E. PubChem 2023 update. *Nucleic Acids Research*, 2023.

Kingma, D. P. and Welling, M. Auto-encoding variational bayes. In *International Conference on Learning Representations*, 2013.

Landrum, G. Fingerprints in the RDKit. In *RDKit User Group Meeting 2012*, 2012. URL https://www.rdkit.org/UGM/2012/Landrum_RDKit_UGM.Fingerprints.Final.pptx.pdf.

Lee, S., Kreis, K., Veccham, S., Liu, M., Reidenbach, D., Paliwal, S., Vahdat, A., and Nie, W. Molecule generation with fragment retrieval augmentation. In *Advances in Neural Information Processing Systems*, 2024.

Lee, S., Kreis, K., Veccham, S. P., Liu, M., Reidenbach, D., Peng, Y., Paliwal, S., Nie, W., and Vahdat, A. GenMol: A drug discovery generalist with discrete diffusion. In *International Conference on Machine Learning*, 2025.

Lewis, P., Perez, E., Piktus, A., Petroni, F., Karpukhin, V., Goyal, N., Küttrler, H., Lewis, M., Yih, W.-t., Rocktäschel, T., et al. Retrieval-augmented generation for knowledge-intensive nlp tasks. *Advances in neural information processing systems*, 33:9459–9474, 2020.

Liu, G., Chen, J., Zhu, Y., Sun, M., Luo, T., Chawla, N. V., and Jiang, M. Graph diffusion transformers are in-context molecular designers. *arXiv:2510.08744*, 2025.

Lo, A., Coley, C. W., and Matusik, W. A genetic algorithm for navigating synthesizable molecular spaces. *arXiv preprint arXiv:2509.20719*, 2025.

Lu, Q., Polyzos, K. D., Li, B., and Giannakis, G. B. Surrogate modeling for bayesian optimization beyond a single gaussian process. *IEEE Transactions on Pattern Analysis and Machine Intelligence*, 45(9):11283–11296, 2023.

McGregor, M. J. and Muskal, S. M. Pharmacophore fingerprinting. 1. application to qsar and focused library design. *Journal of chemical information and computer sciences*, 39(3):569–574, 1999.

Moss, H., Leslie, D., Beck, D., Gonzalez, J., and Rayson, P. BOSS: Bayesian optimization over string spaces. *Advances in neural information processing systems*, 2020.

Moss, H., Ober, S. W., and Diethé, T. Return of the latent space COWBOYS: Re-thinking the use of VAEs for Bayesian optimisation of structured spaces. In *International Conference on Machine Learning*, 2025.

Mukherjee, D., Zhuang, C., Lu, Y., Fu, T., and Zhang, R. Gradient GA: Gradient genetic algorithm for drug molecular design. *Transactions on Machine Learning Research*, 2025.

Navratil, J., Ross, J., Das, P., Mroueh, Y., Hoffman, S. C., Chenthamarakshan, V., and Belgodere, B. GP-MoLFormer-Sim: Test time molecular optimization through contextual similarity guidance. In *Annual AAAI Conference on Artificial Intelligence*, 2026.

Nguyen, T. and Grover, A. LICO: Large language models for in-context molecular optimization. In *International Conference on Learning Representations*, 2025.

Olivecrona, M., Blaschke, T., Engkvist, O., and Chen, H. Molecular de-novo design through deep reinforcement learning. *Journal of cheminformatics*, 9(1):48, 2017.

OpenAI. GPT-5 system card, 2025. URL <https://cdn.openai.com/gpt-5-system-card.pdf>.

Orsi, M. and Reymond, J.-L. One chiral fingerprint to find them all. *Journal of cheminformatics*, 16(1):53, 2024.

Radford, A., Kim, J. W., Hallacy, C., Ramesh, A., Goh, G., Agarwal, S., Sastry, G., Askell, A., Mishkin, P., Clark, J., et al. Learning transferable visual models from natural language supervision. In *International Conference on Machine Learning*, 2021.

Rogers, D. and Hahn, M. Extended-connectivity fingerprints. *Journal of chemical information and modeling*, 50(5):742–754, 2010.

Seidl, P., Vall, A., Hochreiter, S., and Klambauer, G. Enhancing activity prediction models in drug discovery with the ability to understand human language. In *International Conference on Machine Learning*, 2023.

Stokes, J. M., Yang, K., Swanson, K., Jin, W., Cubillos-Ruiz, A., Donghia, N. M., MacNair, C. R., French, S., Carfrae, L. A., Bloom-Ackermann, Z., Tran, V.-A., Chiappino-Pepe, A., Badran, A. H., Andrews, I. W., Chory, E., Church, G. M., Brown, E. D., Jaakkola, T. S., Barzilay, R., and Collins, J. J. A deep learning approach to antibiotic discovery. *Cell*, 180(4):688–702.e13, 2020. doi: 10.1016/j.cell.2020.01.021.

Tripp, A. and Hernández-Lobato, J. M. Genetic algorithms are strong baselines for molecule generation. *arXiv:2310.09267*, 2023.

Tripp, A. and Hernández-Lobato, J. M. Diagnosing and fixing common problems in bayesian optimization for molecule design. *ICML 2024 AI for Science Workshop*, 2024.

Tripp, A., Simm, G. N., and Hernández-Lobato, J. M. A fresh look at de novo molecular design benchmarks. In *NeurIPS 2021 AI for Science Workshop*, 2021.

Wang, H., Skreta, M., Ser, C.-T., Gao, W., Kong, L., Strieth-Kalthoff, F., Duan, C., Zhuang, Y., Yu, Y., Zhu, Y., Du, Y., Aspuru-Guzik, A., Neklyudov, K., and Zhang, C. Efficient evolutionary search over chemical space with large language models. In *International Conference on Learning Representations*, 2025a.

Wang, X., Bi, J., and Song, M. Leveraging partial smiles validation scheme for enhanced drug design in reinforcement learning frameworks. *arXiv preprint arXiv:2505.00530*, 2025b.

Wang-Henderson, M., Soyuer, B., Kassraie, P., Krause, A., and Bogunovic, I. Graph neural bayesian optimization for virtual screening. In *NeurIPS 2023 Workshop on Adaptive Experimental Design and Active Learning in the Real World*, 2023.

Weininger, D. SMILES, a chemical language and information system. 1. introduction to methodology and encoding rules. *Journal of chemical information and computer sciences*, 1988.

Xie, Y., Shi, C., Zhou, H., Yang, Y., Zhang, W., Yu, Y., and Li, L. Mars: Markov molecular sampling for multi-objective drug discovery. In *International Conference on Learning Representations*, 2021.

Xu, P., Fu, T., Gao, W., and Sun, J. Reinvent-transformer: Molecular de novo design through transformer-based reinforcement learning. In *KDD 2024 Workshop on Artificial Intelligence and Data Science for Healthcare: Bridging Data-Centric AI and People-Centric Healthcare*, 2024.

Yong, A., Tripp, A., Hosseini-Gerami, L., and Paige, B. Bayesian optimization for molecules should be pareto-aware. *arXiv preprint arXiv:2507.13704*, 2025.

A. Experimental Details

A.1. Hyperparameters

Table 4 summarizes the hyperparameters used in our experiments. The hyperparameters for MOLLEO and Tripp’s GP BO, which are based on the implementation of MOLLIBRA, are also summarized. Since MOLLEO does not have a pre-evaluation mechanism, it evaluates all generated molecules with the oracle ($N_{\text{batch}} = N_{\text{pairs}} \cdot N_{\text{siblings}}$) and does not use a candidate pool ($N_{\text{cand}} = 0$). Also, considering the limited budget of $N = 1,000$ evaluations, we set $N_{\text{batch}} = 10$ in MOLLEO to reduce the number of oracle calls per generation (originally $N_{\text{batch}} = 70$ in the official code³). On the other hand, MOLLIBRA and Tripp’s GP BO utilize the pre-evaluation mechanism: we set $N_{\text{pairs}} \cdot N_{\text{siblings}} = 50$ and $N_{\text{cand}} = 300$ to ensure candidate diversity, and we use $N_{\text{batch}} = 1$ to increase the number of feedback iterations.

A.2. Prompt Template and Task Descriptions

List. 1 shows the prompt template used for LLM-based molecular editing in MOLLIBRA- \mathcal{L} . We adopt a structured prompt (Berryman & Ziegler, 2024) based on the original template in the official code of MOLLEO. We use this prompt template for both MOLLIBRA- \mathcal{L} and MOLLEO.

Table 5 lists the task classification and task descriptions used in the prompt templates and CLAMP text inputs. The categories are (i) drug-effect optimization, (ii) property optimization, and (iii) structure-based optimization. For (i) drug-effect tasks, which are originally synthetic tasks that maximize similarity to known drug molecules, we reinterpret them as searching for molecules with similar effects or activities to known drugs. In the task descriptions, we only include descriptions of the desired effects or activities⁴. For (ii) property optimization tasks, the names of the subject properties are included in the task descriptions. For (iii), structure-based tasks aim to search for molecules that satisfy structural constraints. For the structure-based tasks, defining a meaningful pharmacological description is non-trivial; thus we explicitly state in the LLM prompt that the task is a black-box function, and the task description a is set to an empty string.

The median_1 task aims to generate molecules with intermediate structures between menthol and camphor; therefore, the effects of both are listed. The median_2 task aims to generate molecules with intermediate structures between tadalafil and sildenafil, and both have the same effect.

³<https://github.com/zoom-wang112358/MOLLEO/tree/main>

⁴MOLLEO (Wang et al., 2025a) and MT-MOL (Kim et al., 2025) included specific drug names in their LLM prompts.

Table 4. Hyperparameters.

Parameter	MOLLEO	MOLLIBRA and GP BO
Initial samples N_{init}	10	10
Population size N_{elite}	30	30
Number of pairs N_{pairs}	10	10
Number of siblings per pair N_{siblings}	1	5
Batch size N_{batch}	10	1
Candidate pool size N_{cand}	0	300

```

1 system_prompt = "You are an expert medicinal chemist
2   collaborating on molecular design. Given scored
3   exemplars, design a new molecule that could
4   outperform them."
5
6 user_prompt_template = """
7   "description": "You are given two candidate molecules
8   and their scores from an optimization oracle
9   derived from multiple medicinal chemistry
10  heuristics. {TASK_DESC}",
11  "candidates": [
12    {
13      "smiles": "{PARENT1_SMILES}",
14      "score": {PARENT1_SCORE}
15    },
16    {
17      "smiles": "{PARENT2_SMILES}",
18      "score": {PARENT2_SCORE}
19    }
20  ],
21  "instructions": "Please propose a chemically valid,
22  synthesizable molecule that should achieve a higher
23  desirability score while balancing exploration of
24  new chemotypes with refinement around promising
25  motifs. Generate {NUM_SIBLINGS} distinct candidate
26  molecules. Each entry must use SMILES and all
27  candidates must be returned in the 'smiles' field.
28  Respond with a single JSON object containing only
29  the key 'smiles' mapped to an array of exactly {
30  NUM_SIBLINGS} unique SMILES strings. Do not include
31  any additional narrative text."
32 }
33 """

```

Listing 1. Prompt template used in EDITMOL subroutine for MOLLIBRA- \mathcal{L} and MOLLEO.

B. Additional Experimental Results

B.1. Additional analysis of critic contributions

Figure 4 shows the critic contributions during the optimization process of MOLLIBRA- \mathcal{G} . Figure 5 presents heatmaps of critic contributions for different random seeds in two tasks.

B.2. Comparison with Latent-space Optimization Methods

Table 6 presents the Top-10 AUC comparison under the PMO-300 budget ($N = 300$ oracle calls) with latent-space optimization methods including COWBOYS (Moss et al., 2025). GA (Genetic Algorithm), CMA-ES, Random Line BO, and TURBO are general optimization methods, and they have been evaluated as applications to molecu-

Table 5. Task descriptions for LLM prompt templates and CLAMP text inputs.

	{TASK_DESC} in List. 1	Task description for CLAMP: <i>a</i>
Drug effect optimization		
albuterol_similarity	The oracle rewards molecules that act as beta-2 adrenergic receptor agonists.	Beta-2 adrenergic receptor agonists
amlodipine_mpo	The oracle rewards molecules that inhibit the L-type calcium channel.	Inhibition of the L-type calcium channel
celecoxib_rediscovery	The oracle rewards molecules that inhibit cyclooxygenase-2.	Inhibition of cyclooxygenase-2
drd2_docking	The oracle rewards molecules that act as dopamine D2 receptor ligands.	Dopamine D2 receptor ligand
fenofenadine_mpo	The oracle rewards molecules that inhibit the histamine H1 receptor.	Inhibition of the histamine H1 receptor
gsk3_beta	The oracle rewards molecules that inhibit glycogen synthase kinase-3-beta.	Inhibition of glycogen synthase kinase-3-beta
jnk3	The oracle rewards molecules that inhibit c-Jun N-terminal kinase 3.	Inhibition of c-Jun N-terminal kinase 3
median_1	This oracle rewards molecules that act as TRPV3/TRPM8 agonists.	Agonism of human TRPV3/TRPM8
median_2	This oracle rewards molecules that inhibit PDE5A catalytic activity.	Inhibition of recombinant human PDE5A catalytic activity
mestranol_similarity	The oracle rewards molecules that inhibit estrogen receptor binding activity.	Inhibition of estrogen receptor binding activity
osimetrinib_mpo	The oracle rewards molecules that inhibit EGFR tyrosine kinase activity.	Inhibition of EGFR tyrosine kinase activity
perindopril_mpo	The oracle rewards molecules that inhibit the angiotensin-converting enzyme.	Inhibition of the angiotensin-converting enzyme
ranolazine_mpo	The oracle rewards molecules that inhibit late sodium current.	Inhibition of late sodium current
sitagliptin_mpo	The oracle rewards molecules that inhibit dipeptidyl peptidase 4 enzyme activity.	Inhibition of dipeptidyl peptidase 4 enzyme activity
thiothixene_rediscovery	The oracle rewards molecules that act as dopamine D2 receptor antagonists.	Dopamine D2 receptor antagonists
troglitazone_rediscovery	The oracle rewards molecules that act as human peroxisome proliferator-activated receptor gamma agonists.	Human peroxisome proliferator-activated receptor gamma agonists
zaleplon_mpo	The oracle rewards molecules that act as Gamma-Aminobutyric Acid A receptor agonists.	Gamma-Aminobutyric Acid A receptor agonists
Property optimization		
rdkit_qed	The oracle returns the Quantitative Estimate of Drug-likeness (QED) normalized to [0,1]; higher values indicate a more drug-like profile. External tool invocation is prohibited.	Quantitative Estimate of Drug-likeness (QED)
Structure-based optimization		
deco_hop	This oracle is a black-box function; its analytical form is unavailable and it can only be probed via oracle evaluations.	N/A (input empty string)
scaffold_hop		
isomer_c7h8n2o2		
isomer_c9h10n2o2pf2cl		

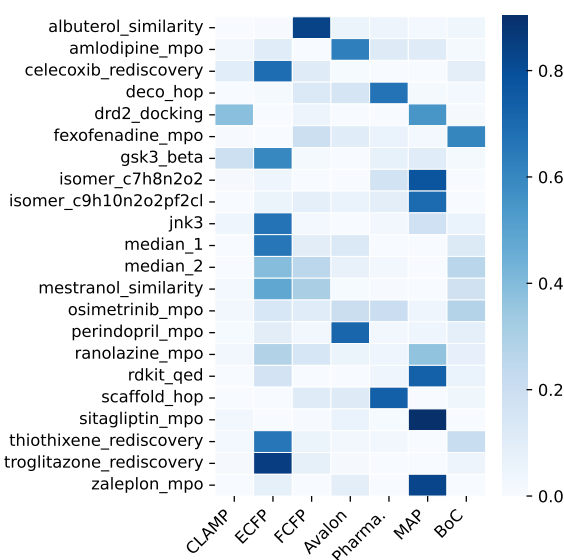


Figure 4. Heatmap of critic contributions during the optimization process of MOLLIBRA-*G*. Compared to MOLLIBRA-*L* shown in Figure 2, the dominant critics for each task are generally consistent.

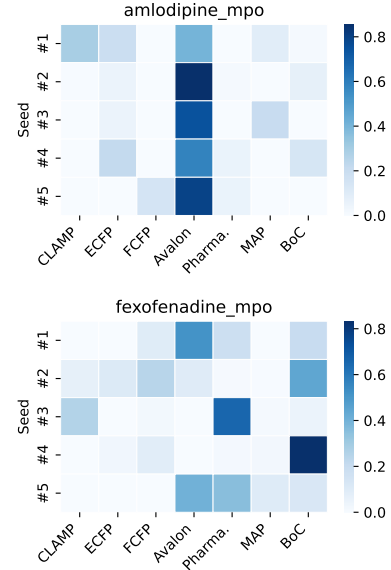


Figure 5. Heatmaps showing the critic contributions for different seeds. While amlodipine_mpo shows consistent critic contributions across seeds, fenofenadine_mpo exhibits large variation depending on the seed.

lar optimization in latent space by [González-Duque et al. \(2024\)](#). All latent-space optimization results in Table 6 are evaluated using the COWBOYS codebase⁵. Although the prior latent-space studies report effectiveness on PMO-300, MOLLIBRA outperforms latent-space optimization methods even in this low-budget setting.

B.3. Additional Ablation Study

Ensemble method for GPs This section presents an ablation study on the GP ensemble method. Table 7 shows the comparison with Product of Experts (PoE) ([Cao & Fleet, 2014](#)) as an alternative to the selection-based ensemble method ([Lu et al., 2023](#)) that we use in the main text. Comparing the Sum row, the selection method outperforms PoE. The difference is small but consistent in both MOLLIBRA- \mathcal{G} and MOLLIBRA- \mathcal{L} ; therefore, we adopted the selection method in the main text. A possible reason for the similar results is that both the selection method and PoE assign dynamic weights to the GPs. PoE takes the product of the predictive distributions of each GP (i.e., $\prod_{m=1}^M \mathcal{N}(f; \mu_m, \sigma_m^2)$) as the ensemble result, which is equivalent to a weighted average of the predictive means $\{\mu_m\}$ with weights based on the precisions $\{\sigma_m^{-2}\}$.

Gating method for CLAMP This section presents an ablation study on the gating method for the CLAMP critic. Table 8 shows the comparison results with EXP3 ([Auer et al., 2002](#)) and LLIMBO ([Chang et al., 2025](#)) as alternatives to the correlation-based gating method that we use. EXP3 is a multi-armed bandit algorithm, and here it learns the gating probabilities using score improvement as rewards. Since the improvements are rarely observed, the learning speed tends to be slow, resulting in EXP3 performing the worst in both MOLLIBRA- \mathcal{G} and MOLLIBRA- \mathcal{L} . LLIMBO is an algorithm for combining candidates proposed by a GP and LLM in general black-box optimization formulations. In this paper, LLIMBO computes the quantile of the CLAMP-proposed candidate among all candidates ranked by the GP critics, and then uses that quantile as the gating probability⁶. Although this method is competitive with the correlation-based method in both MOLLIBRA- \mathcal{G} and MOLLIBRA- \mathcal{L} , we adopted the correlation-based method in the main text because of its simplicity.

B.4. Wall-clock Time and API Call Cost

Table 9 presents the wall-clock time and API call cost comparison on the PMO-1K benchmark. We run GP training/in-

ference and CLAMP evaluation on an NVIDIA H200 GPU. Since MOLLIBRA uses multiple critics, it is computationally more expensive than Tripp’s GP BO, which uses a single critic; however, the increase in time per iteration is only a few seconds. While MOLLIBRA- \mathcal{L} incurs approximately $20\times$ the API call cost compared to MOLLEO, the total cost per seed is about USD 5.

⁵<https://github.com/henrymoss/ROTLSC/tree/main>

⁶This method is a modification of LLIMBO-Justify proposed in the original paper ([Chang et al., 2025](#)), adapted to probabilistically select whether to adopt CLAMP or not.

Table 6. Top-10 AUC comparison on PMO-300 with latent-space optimization methods in the low budget regime.

	GA	CMA-ES (González-Duque et al., 2024)	Random Line BO	TURBO	COWBOYS (Moss et al., 2025)	MOLLIBRA- \mathcal{G} (ours)	MOLLIBRA- \mathcal{L} (ours)
Latent-space optimization	✓	✓	✓	✓	✓		
albuterol_similarity	0.321 \pm 0.024	0.330 \pm 0.041	0.347 \pm 0.036	0.357 \pm 0.040	0.357 \pm 0.034	0.748 \pm 0.021	0.890 \pm 0.043
amlodipine_mpo	0.426 \pm 0.014	0.386 \pm 0.009	0.387 \pm 0.010	0.374 \pm 0.015	0.392 \pm 0.013	0.488 \pm 0.041	0.508 \pm 0.045
celecoxib_rediscovery	0.197 \pm 0.006	0.176 \pm 0.007	0.176 \pm 0.009	0.167 \pm 0.006	0.192 \pm 0.019	0.366 \pm 0.026	0.588 \pm 0.073
deco_hop	0.557 \pm 0.006	0.538 \pm 0.004	0.541 \pm 0.009	0.536 \pm 0.003	0.546 \pm 0.010	0.591 \pm 0.010	0.597 \pm 0.012
drd2_docking	0.064 \pm 0.082	0.034 \pm 0.015	0.095 \pm 0.064	0.051 \pm 0.023	0.079 \pm 0.082	0.669 \pm 0.294	0.912 \pm 0.029
fenofenadine_mpo	0.544 \pm 0.036	0.585 \pm 0.027	0.612 \pm 0.019	0.594 \pm 0.014	0.598 \pm 0.016	0.689 \pm 0.039	0.689 \pm 0.040
gsk3_beta	0.159 \pm 0.025	0.179 \pm 0.016	0.238 \pm 0.073	0.160 \pm 0.016	0.222 \pm 0.021	0.333 \pm 0.054	0.564 \pm 0.050
isomer_c7h8n2o2	0.592 \pm 0.106	0.601 \pm 0.066	0.578 \pm 0.070	0.517 \pm 0.079	0.666 \pm 0.081	0.751 \pm 0.015	0.713 \pm 0.069
isomer_c9h10n2o2pf2cl	0.477 \pm 0.023	0.401 \pm 0.061	0.470 \pm 0.095	0.444 \pm 0.055	0.444 \pm 0.054	0.653 \pm 0.108	0.564 \pm 0.270
jnk3	0.085 \pm 0.009	0.074 \pm 0.009	0.077 \pm 0.011	0.080 \pm 0.010	0.083 \pm 0.008	0.234 \pm 0.070	0.297 \pm 0.107
median_1	0.131 \pm 0.014	0.121 \pm 0.004	0.124 \pm 0.019	0.121 \pm 0.005	0.162 \pm 0.032	0.279 \pm 0.011	0.225 \pm 0.030
median_2	0.142 \pm 0.011	0.126 \pm 0.004	0.126 \pm 0.004	0.124 \pm 0.006	0.135 \pm 0.008	0.193 \pm 0.026	0.230 \pm 0.018
mestranol_similarity	0.250 \pm 0.031	0.287 \pm 0.022	0.299 \pm 0.020	0.302 \pm 0.028	0.330 \pm 0.016	0.477 \pm 0.084	0.470 \pm 0.020
osimetrinib_mpo	0.672 \pm 0.036	0.597 \pm 0.027	0.596 \pm 0.018	0.600 \pm 0.041	0.639 \pm 0.007	0.708 \pm 0.024	0.750 \pm 0.039
perindopril_mpo	0.321 \pm 0.110	0.229 \pm 0.031	0.265 \pm 0.037	0.235 \pm 0.053	0.255 \pm 0.033	0.455 \pm 0.026	0.483 \pm 0.024
ranolazine_mpo	0.299 \pm 0.081	0.420 \pm 0.026	0.378 \pm 0.129	0.378 \pm 0.053	0.481 \pm 0.030	0.653 \pm 0.012	0.689 \pm 0.029
rdkit_qed	0.884 \pm 0.031	0.823 \pm 0.029	0.820 \pm 0.037	0.816 \pm 0.019	0.817 \pm 0.021	0.903 \pm 0.014	0.923 \pm 0.006
scaffold_hop	0.421 \pm 0.009	0.397 \pm 0.017	0.406 \pm 0.014	0.392 \pm 0.007	0.410 \pm 0.007	0.483 \pm 0.002	0.484 \pm 0.013
sitagliptin_mpo	0.119 \pm 0.071	0.099 \pm 0.034	0.152 \pm 0.066	0.074 \pm 0.013	0.186 \pm 0.067	0.236 \pm 0.063	0.298 \pm 0.056
thiothixene_rediscovery	0.218 \pm 0.014	0.195 \pm 0.008	0.195 \pm 0.005	0.194 \pm 0.008	0.200 \pm 0.019	0.326 \pm 0.036	0.480 \pm 0.079
troglitazone_rediscovery	0.181 \pm 0.016	0.160 \pm 0.007	0.158 \pm 0.008	0.160 \pm 0.003	0.170 \pm 0.006	0.316 \pm 0.031	0.310 \pm 0.030
zaleplon_mpo	0.278 \pm 0.087	0.225 \pm 0.021	0.283 \pm 0.037	0.216 \pm 0.044	0.259 \pm 0.052	0.386 \pm 0.026	0.394 \pm 0.053
Sum	7.339	6.983	7.319	6.892	7.621	10.934	12.058

Table 7. Ablation study results on the GP ensemble method (Top-10 AUC on PMO-300), comparing the selection method (Lu et al., 2023) used in the main text and PoE (Cao & Fleet, 2014).

GP ensemble	MOLLIBRA- \mathcal{G}		MOLLIBRA- \mathcal{L}	
	Selection	PoE	Selection	PoE
albuterol_similarity	0.748 \pm 0.021	0.741 \pm 0.085	0.890 \pm 0.043	0.900 \pm 0.055
amlodipine_mpo	0.488 \pm 0.041	0.496 \pm 0.053	0.508 \pm 0.045	0.527 \pm 0.049
celecoxib_rediscovery	0.366 \pm 0.026	0.378 \pm 0.021	0.588 \pm 0.073	0.484 \pm 0.059
deco_hop	0.591 \pm 0.010	0.593 \pm 0.011	0.597 \pm 0.012	0.601 \pm 0.012
drd2_docking	0.669 \pm 0.294	0.643 \pm 0.290	0.912 \pm 0.029	0.876 \pm 0.038
fenofenadine_mpo	0.689 \pm 0.039	0.664 \pm 0.066	0.689 \pm 0.040	0.672 \pm 0.061
gsk3_beta	0.333 \pm 0.054	0.356 \pm 0.055	0.564 \pm 0.050	0.571 \pm 0.029
isomer_c7h8n2o2	0.751 \pm 0.015	0.725 \pm 0.090	0.713 \pm 0.069	0.612 \pm 0.089
isomer_c9h10n2o2pf2cl	0.653 \pm 0.108	0.636 \pm 0.085	0.564 \pm 0.270	0.676 \pm 0.103
jnk3	0.234 \pm 0.070	0.222 \pm 0.057	0.297 \pm 0.107	0.337 \pm 0.034
median_1	0.279 \pm 0.011	0.281 \pm 0.013	0.225 \pm 0.030	0.221 \pm 0.049
median_2	0.193 \pm 0.026	0.192 \pm 0.021	0.230 \pm 0.018	0.218 \pm 0.017
mestranol_similarity	0.477 \pm 0.084	0.414 \pm 0.042	0.470 \pm 0.020	0.455 \pm 0.045
osimetrinib_mpo	0.708 \pm 0.024	0.692 \pm 0.048	0.750 \pm 0.039	0.756 \pm 0.067
perindopril_mpo	0.455 \pm 0.026	0.442 \pm 0.022	0.483 \pm 0.024	0.459 \pm 0.012
ranolazine_mpo	0.653 \pm 0.012	0.656 \pm 0.028	0.689 \pm 0.029	0.697 \pm 0.015
rdkit_qed	0.903 \pm 0.014	0.909 \pm 0.014	0.923 \pm 0.006	0.915 \pm 0.017
scaffold_hop	0.483 \pm 0.002	0.492 \pm 0.012	0.484 \pm 0.013	0.483 \pm 0.016
sitagliptin_mpo	0.236 \pm 0.063	0.213 \pm 0.078	0.298 \pm 0.056	0.322 \pm 0.087
thiothixene_rediscovery	0.326 \pm 0.036	0.370 \pm 0.037	0.480 \pm 0.079	0.430 \pm 0.034
troglitazone_rediscovery	0.316 \pm 0.031	0.309 \pm 0.020	0.310 \pm 0.030	0.301 \pm 0.038
zaleplon_mpo	0.386 \pm 0.026	0.368 \pm 0.047	0.394 \pm 0.053	0.401 \pm 0.068
Sum	10.934	10.791	12.058	11.912

Table 8. Ablation study results on the CLAMP gating method (Top-10 AUC on PMO-300), comparing the correlation-based method (denoted as Corr.) used in the main text with LLIMBO (Chang et al., 2025) and EXP3 (Auer et al., 2002).

CLAMP gating	MOLLIBRA- \mathcal{G}			MOLLIBRA- \mathcal{L}		
	Corr.	LLIMBO	EXP3	Corr.	LLIMBO	EXP3
albuterol_similarity	0.748 \pm 0.021	0.745 \pm 0.036	0.718 \pm 0.085	0.890 \pm 0.043	0.912 \pm 0.019	0.893 \pm 0.027
amlodipine_mpo	0.488 \pm 0.041	0.483 \pm 0.059	0.456 \pm 0.051	0.508 \pm 0.045	0.541 \pm 0.039	0.520 \pm 0.051
celecoxib_rediscovery	0.366 \pm 0.026	0.392 \pm 0.052	0.343 \pm 0.015	0.588 \pm 0.073	0.497 \pm 0.069	0.496 \pm 0.102
deco_hop	0.591 \pm 0.010	0.599 \pm 0.010	0.597 \pm 0.008	0.597 \pm 0.012	0.605 \pm 0.019	0.604 \pm 0.015
drd2_docking	0.669 \pm 0.294	0.755 \pm 0.132	0.650 \pm 0.347	0.912 \pm 0.029	0.911 \pm 0.023	0.930 \pm 0.015
fexofenadine_mpo	0.689 \pm 0.039	0.656 \pm 0.042	0.645 \pm 0.052	0.689 \pm 0.040	0.674 \pm 0.051	0.664 \pm 0.047
gsk3_beta	0.333 \pm 0.054	0.352 \pm 0.066	0.315 \pm 0.048	0.564 \pm 0.050	0.556 \pm 0.105	0.551 \pm 0.055
isomer_c7h8n2o2	0.751 \pm 0.015	0.784 \pm 0.027	0.653 \pm 0.060	0.713 \pm 0.069	0.660 \pm 0.066	0.555 \pm 0.236
isomer_c9h10n2o2pf2cl	0.653 \pm 0.108	0.659 \pm 0.070	0.575 \pm 0.067	0.564 \pm 0.270	0.618 \pm 0.140	0.416 \pm 0.254
jnk3	0.234 \pm 0.070	0.207 \pm 0.039	0.225 \pm 0.050	0.297 \pm 0.107	0.356 \pm 0.092	0.324 \pm 0.114
median_1	0.279 \pm 0.011	0.272 \pm 0.024	0.255 \pm 0.014	0.225 \pm 0.030	0.213 \pm 0.029	0.196 \pm 0.015
median_2	0.193 \pm 0.026	0.191 \pm 0.022	0.185 \pm 0.021	0.230 \pm 0.018	0.212 \pm 0.010	0.210 \pm 0.018
mestranol_similarity	0.477 \pm 0.084	0.469 \pm 0.040	0.473 \pm 0.052	0.470 \pm 0.020	0.444 \pm 0.038	0.415 \pm 0.035
osimetrinib_mpo	0.708 \pm 0.024	0.724 \pm 0.018	0.679 \pm 0.057	0.750 \pm 0.039	0.768 \pm 0.029	0.741 \pm 0.045
perindopril_mpo	0.455 \pm 0.026	0.448 \pm 0.032	0.420 \pm 0.014	0.483 \pm 0.024	0.486 \pm 0.016	0.469 \pm 0.024
ranolazine_mpo	0.653 \pm 0.012	0.670 \pm 0.022	0.649 \pm 0.039	0.689 \pm 0.029	0.701 \pm 0.016	0.680 \pm 0.020
rdkit_qed	0.903 \pm 0.014	0.904 \pm 0.015	0.896 \pm 0.018	0.923 \pm 0.006	0.909 \pm 0.024	0.922 \pm 0.008
scaffold_hop	0.483 \pm 0.002	0.484 \pm 0.008	0.474 \pm 0.005	0.484 \pm 0.013	0.487 \pm 0.013	0.475 \pm 0.013
sitagliptin_mpo	0.236 \pm 0.063	0.149 \pm 0.079	0.195 \pm 0.064	0.298 \pm 0.056	0.313 \pm 0.092	0.264 \pm 0.111
thiothixene_rediscovery	0.326 \pm 0.036	0.332 \pm 0.013	0.291 \pm 0.021	0.480 \pm 0.079	0.449 \pm 0.073	0.405 \pm 0.048
troglitazone_rediscovery	0.316 \pm 0.031	0.302 \pm 0.027	0.317 \pm 0.029	0.310 \pm 0.030	0.318 \pm 0.049	0.282 \pm 0.021
zaleplon_mpo	0.386 \pm 0.026	0.383 \pm 0.034	0.362 \pm 0.014	0.394 \pm 0.053	0.384 \pm 0.032	0.380 \pm 0.046
Sum	10.934	10.960	10.375	12.058	12.015	11.391

Table 9. Wall-clock time and LLM API (GPT-5-mini) call cost comparison on the PMO-1K benchmark. These results are averaged over 5 seeds on the albuterol_similarity task.

Method	Total time	Avg. time per iter.	Total API cost
MOLLIBRA- \mathcal{G}	3.32h	11.95s	-
MOLLIBRA- \mathcal{L}	4.22h	15.19s	4.88 USD
Tripp's GP	2.34h	8.42s	-
MOLLEO	16.4 min	0.99s	0.25 USD